Suplemento de la Revista Mexicana de Física **3** 0308113 (2022) 1–5

On wide-angle photo- and electroproduction of pions to twist-3 accuracy

K. Passek-Kumerički

Division of Theoretical Physics, Rudjer Bošković Institute, HR-10002 Zagreb, Croatia.
Presented at HADRON2021.

Received 22 January 2022; accepted 12 March 2022

The wide-angle photo- and electroproduction of pions is investigated within the handbag mechanism in which the $\gamma^{(*)}N \to \pi N'$ amplitudes factorize into subprocess amplitudes,$\gamma^{(*)}q \to \pi q'$, and form factors representing $1/x$-moments of generalized parton distributions (GPDs). The subprocess is calculated to twist-3 accuracy taking into account both the 2- and 3-body Fock components of the pion. The cross-sections are compared to experiment and spin-effects are discussed.

Keywords: Exclusive processes; meson production; generalized parton distributions; distribution amplitudes; higher twist.

DOI: https://doi.org/10.31349/SuplRevMexFis.3.0308113

1. Introduction

The hard exclusive processes are successfully described by the handbag mechanism in which only one quark from the incoming nucleon and one from the outgoing nucleon participate in the hard subprocess while all other partons are spectators. In particular, it was applied to the Compton scattering $\gamma^{(*)}N \to \gamma N$, the simplest probe of the nucleon structure, as well as, to the meson electroproduction $\gamma^{(*)}N \to MN'$. The prerequisite of this approach is the existence of at least one large scale in the process enabling the use of the perturbative expansion in the strong coupling constant, as well as, the twist expansion. Two kinematical regions were extensively investigated in the past. The deeply virtual (DV) region is characterized by the large virtuality Q^2 of the incoming photon and a small momentum transfer $(-t)$ from the incoming to the outgoing nucleon. In the wide-angle (WA) region $(-t)$ is large, as well as $(-u)$ and s, while Q^2 is smaller than $(-t)$ ($Q^2 = 0$ in the case of photoproduction). The all order proofs of factorization exist for DV Compton scattering (DVCS) [1] and DV meson production (DVMP) [2]. The process amplitudes factorize in hard perturbatively calculable subprocess amplitudes and generalized parton distributions (GPDs) which encapsulate the soft hadron-parton transitions, *i.e.*, and the hadron structure. In contrast, for WA processes the general factorization proofs are still missing but it was shown that the factorization holds to next-to-leading order in the strong coupling for WA Compton scaterring (WACS) [3, 4] and to leading-order for WA meson production (WAMP) [5]. In these cases it was argued that in the symmetric frame where skewness is zero the process amplitudes can be represented as a product of subprocess amplitudes and form factors that represent $1/x$ moments of GPDs at zero-skewness.

Both DVCS and WACS were widely investigated in the last decades and the handbag factorization achieved a good description of the experimental data. But for the DV pion production the experimental data indicate the importance of the transversely polarized virtual photons [6–9] and the need to go beyond the leading twist-2 calculation since only the longitudinally polarized photons contribute to the latter. The twist-3 calculation with transversity GPDs was proposed and the calculation including twist-3 2-body pion Fock component achieved already the successful agreement with the data [10]. Similarly, the experimental data for photoproduction [11–13] show that the the twist-2 contributions for WA pion production [5] are not sufficient. In contrast to DVMP, it was found that the twist-3 contribution to pion photoproduction vanishes in often used Windzura-Wilczek approximation, i.e., when just twist-3 2-body pion Fock components are considered [14]. Both 2- and 3-body twist-3 Fock components of π_0 were considered in [15] and the results were successfully fitted to CLAS data [11]. We report here on extension of this work to the twist-3 prediction for $P = \pi^{\pm}, \pi^0$ WA photo- and electroproduction [16].

2. Application of handbag mechanism

The helicity amplitudes $\mathcal{M}^P_{\nu,\kappa',\mu,\kappa}$ for $\gamma^{(*)}(\mu)N(\kappa) \to P(\nu)N'(\kappa')$ process, *i.e.*, the (electro)production of the pseudoscalar meson P, in the WA angle region can be expressed as

$$\begin{aligned}
\mathcal{M}^P_{0+,\mu+} &= \frac{e_0}{2}\sum_\lambda \Big[\mathcal{H}^P_{0\lambda,\mu\lambda}\,\big(R^P_V(t) + 2\lambda\, R^P_A(t)\big) \\
&\quad - 2\lambda\,\frac{\sqrt{-t}}{2m}\,\mathcal{H}^P_{0-\lambda,\mu\lambda}\,\bar{S}^P_T(t)\Big] \\
\mathcal{M}^P_{0-,\mu+} &= \frac{e_0}{2}\sum_\lambda \Big[\frac{\sqrt{-t}}{2m}\,\mathcal{H}^P_{0\lambda,\mu\lambda}\,R^P_T(t) \\
&\quad - 2\lambda\,\frac{t}{2m^2}\,\mathcal{H}^P_{0-\lambda,\mu\lambda}\,S^P_S(t)\Big] \\
&\quad + e_0\mathcal{H}^P_{0-,\mu+}\,S^P_T(t),
\end{aligned} \tag{1}$$

where m is a nucleon mass.

The soft form factors, R^P_i and S^P_i (F^P_i), represent specific flavor combinations of $1/x$-moments of zero-skewness GPDs (K^a_i)

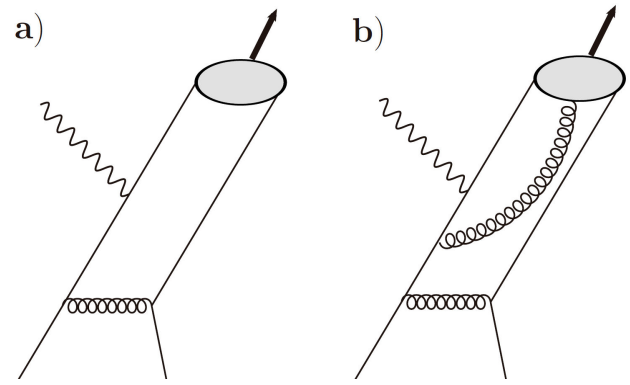

FIGURE 1. Generic diagrams corresponding to the 2- and 3-body subprocess amplitudes.

$$F_i^a(t) = \int_0^1 \frac{dx}{x}\, K_i^a(x,t)\,, \tag{2}$$

where x is the average momentum fraction of an active quark and a is its flavour. The form factors R_V^P, R_A^P and R_T^P are related to the helicity non-flip GPDs H, $\widetilde{H}$ and E, respectively. The S-type form factors, S_T^P, $\bar{S}_T^P$ and S_S^P are related to the helicity-flip or transversity GPDs H_T, $\bar{E}_T$ and $\widetilde{H}_T$, respectively.[i]

The amplitudes $\mathcal{H}_{\mu,\lambda,\nu,\lambda'}$ correspond to the subprocesses $\gamma^{(*)}(\mu)q(\lambda) \to P(\nu)q'(\lambda')$. and they are calculated using handbag diagrams as the ones depicted on Fig. 1. The meson P with momentum q' is replaced by an appropriate 2- or 3-body Fock state. The 2-body projector $\pi \to q\bar{q}$ [17] given by

$$\begin{aligned}\mathcal{P}_2^P \sim f_\pi \Big\{ & \gamma_5 \not{q}' \phi_\pi(\tau,\mu_F) + \mu_\pi(\mu_F)\Big[\gamma_5 \phi_{\pi p}(\tau,\mu_F) \\ & - \frac{i}{6}\gamma_5 \sigma_{\mu\nu}\frac{q'^\mu n^\nu}{q'\cdot n}\phi'_{\pi\sigma}(\tau,\mu_F) \\ & + \frac{i}{6}\gamma_5\sigma_{\mu\nu}\, q'^\mu \phi_{\pi\sigma}(\tau,\mu_F)\frac{\partial}{\partial k_{\perp\nu}}\Big]\Big\}_{k_\perp\to 0}\,, \end{aligned} \tag{3}$$

contributes to the subprocess amplitudes corresponding to the diagrams depicted on Fig. 1a). The quark (antiquark) longitudinal momentum fraction is denoted by τ ($\bar{\tau}$), and k_T represents its intrinsic transverse momentum. The first term in (3) corresponds to the twist-2 part, while the twist-3 part is proportional to the chiral condensate $\mu_\pi = m_\pi^2/(m_u+m_d) \cong 2$ GeV (at the factorization scale $\mu_F = 2$ GeV). This parameter is large and although the twist-3 cross section for pion electroproduction is suppressed by μ_π^2/Q^2 as compared to twist-2 cross section, for the range of Q^2 accessible in current experiments the suppression factor is of order unity.[ii] The 3-body $\pi \to q\bar{q}g$ projector [15]

$$\mathcal{P}_3^P \sim f_{3\pi}(\mu_F)\,\frac{i}{g}\,\gamma_5\,\sigma_{\mu\nu} q'^\mu g_\perp^{\nu\rho}\,\frac{\phi_{3\pi}(\tau_a,\tau_b,\tau_g,\mu_F)}{\tau_g}, \tag{4}$$

contributes to the subprocesses amplitudes corresponding to Fig. 1b). The pion constituents are taken to be collinear to the pion and τ_i denote their longitudinal momentum fractions. The helicity non-flip amplitudes $\mathcal{H}_{0\lambda,\mu,\lambda'}$ are generated by twist-2, while the helicity flip ones $\mathcal{H}_{0-\lambda,\mu,\lambda'}$ are of twist-3 origin.

Similarly to GPDs, the pion distribution amplitudes (DAs) ϕ encode the long distance effects and thus the pion structure. In addition to twist-2 DA ϕ_π there are two 2-body twist-3 DAs, $\phi_{\pi p}$ and $\phi_{\pi\sigma}$, and 3-body twist-3 DA $\phi_{3\pi}$. Twist-3 DAs are connected by equations of motion (EOMs)

$$\begin{aligned}\tau\phi_{\pi p}(\tau) + \frac{\tau}{6}\,\phi'_{\pi\sigma}(\tau) - \frac{1}{3}\,\phi_{\pi\sigma}(\tau) &= \phi_{\pi 2}^{EOM}(\bar{\tau}) \\ \bar{\tau}\phi_{\pi p}(\tau) - \frac{\tau}{6}\phi'_{\pi\sigma}(\tau) - \frac{1}{3}\phi_{\pi\sigma}(\tau) &= \phi_{\pi 2}^{EOM}(\tau), \end{aligned} \tag{5}$$

where

$$\phi_{\pi 2}^{EOM}(\tau) = 2\frac{f_{3\pi}}{f_\pi \mu_\pi}\int_0^{\bar{\tau}} \frac{d\tau_g}{\tau_g}\,\phi_{3\pi}(\tau,\bar{\tau}-\tau_g,\tau_g).$$

Using EOMs and DA symmetry properties the twist-3 subprocess amplitudes can be expressed in terms of just two twist-3 DAs and 2- and 3-body contributions can be combined. Moreover, EOMs lead to the inhomogeneous linear first order differential equation which from known 3-body DA $\phi_{3\pi}$ [18] fixes $\phi_{\pi p}$ (and $\phi_{\pi\sigma}$). We note that in the derivation of $q\bar{q}g$ projector and EOMs the same gauge has to be used for the constituent gluon, and we have consistently used the light-cone gauge.

For meson electroproduction both transverse and longitudinal photons contribute to twist-2 subprocess amplitudes. As expected in photoproduction limit ($Q^2 = 0$) the longitudinal contribution vanishes, while in DVMP limit ($t \to 0$) only the longitudinal photons contribute. The twist-3 contributions both for transverse and longitudinal photons have general structure

$$\begin{aligned}\mathcal{H}^{P,tw3} &= \mathcal{H}^{P,tw3,q\bar{q}} + \mathcal{H}^{P,tw3,q\bar{q}g} \\ &= \big(\mathcal{H}^{P,\phi_{\pi p}} + \underbrace{\mathcal{H}^{P,\phi_{\pi 2}^{EOM}}}\big) + \underbrace{\big(\mathcal{H}^{P,q\bar{q}g,C_F}} + \mathcal{H}^{P,q\bar{q}g,C_G}\big) \\ &= \mathcal{H}^{P,\phi_{\pi p}} + \qquad \mathcal{H}^{P,\phi_{3\pi},C_F} \quad + \mathcal{H}^{P,\phi_{3\pi},C_G}. \end{aligned} \tag{6}$$

The twist-3 2-body contribution $\mathcal{H}^{P,tw3,q\bar{q}}$ is proportional to C_F colour factor, while twist-3 3-body contribution has C_F and C_G proportional parts. The C_G part is separately gauge invariant, while for C_F contributions only the sum of 2- and 3-body parts is gauge invariant (with respect to the choice of photon or virtual gluon gauge). We have used EOMs to obtain that sum, as well as, the complete twist-3 contribution expressed through just two twist-3 DAs, $\phi_{3\pi}$ and $\phi_{\pi p}$. The twist-3 subprocess amplitude for longitudinal photons vanishes both for $Q \to 0$ and $t \to 0$, i.e, for photoproduction and DVMP. One finds that for photoproduction $\mathcal{H}^{P,\phi_{\pi p}} = 0$ [15]. For DVMP $\mathcal{H}^{P,\phi_{\pi 2}^{EOM}} = 0$, and although for $t \neq 0$ one finds no end-point singularities, in this limit one has to deal with end-point singularities in $\mathcal{H}^{P,\phi_{\pi p}}$ [10].

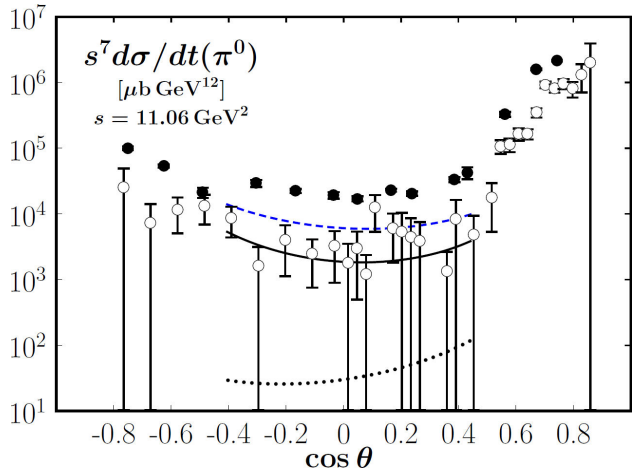

FIGURES 2, 3. 2.- Photoproduction. 3.- The cross section for π^0 photoproduction. The solid (dotted) curve represents the full (twist 2) result. The dashed curve is obtained with the amplitudes taken at the fixed renormalization and factorization scale $\mu_R = \mu_F = 1$ GeV. Data taken CLAS [11] (open circles) and from SLAC [12] (the latter provided at $s = 10.3$ GeV^2).

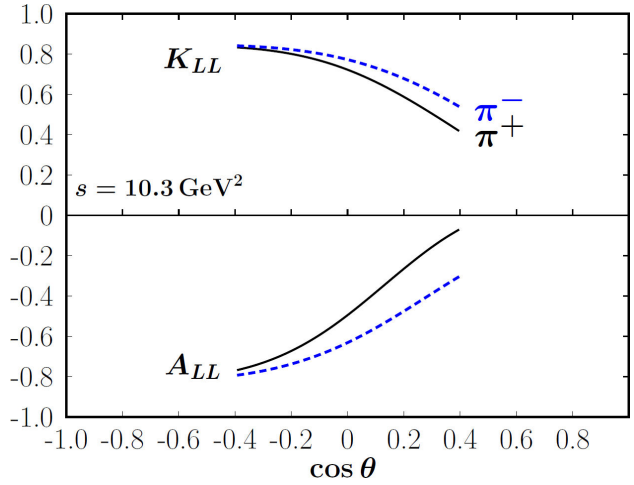

FIGURE 4. Results for the helicity correlation parameters A_{LL} and K_{LL} for π^+ and π^- photoproduction.

3. Numerical results

For details on the form of the pion DAs, GPDs and parameters used to obtain the numerical results as well as the explicit expressions derived for the subprocess amplitudes we refer to [16]. The form factors related to both helicity non-flip and transversity GPDs and only two independent pion DAs (twist-2 pion DA ϕ_π and twist-3 3-body pion DA $\phi_{3\pi}$) remain as soft physics input. The latter are accompanied by decay constants f_π and $f_{3\pi}$.

We comment here on few selected results. In Ref. [15] the cross-section for π^0 photoproduction has been fitted to [11] data. The results are displayed in Fig. 3.

As it was already noted in Ref. [5], one can see from Fig. 3 that twist-2 prediction lies well beyond the data. But by including the twist-3 contributions one obtains reasonable agreement with the experiment. Twist-3 is more important in backward hemisphere (θ is c.m.s. scattering angle). The twist-2 and twist-3 cross sections scale as s^{-7} and s^{-8}, respectively. Our results have effective s^{-9} scaling which is a bit too strong. As an attempt to modify this the fixed renormalization and factorization scales were tested. In Ref. [16] such an analysis was extended to π^+ and π^- for which only few experimental data are available [12, 13], The similar behaviour of photoproduction cross-sections was found.

For pion electroproduction there are four partial cross sections: $d\sigma_L/dt$, $d\sigma_T/dt$, $d\sigma_{LT}/dt$, and $d\sigma_{TT}/dt$. In Ref. [16] the theoretical predictions were given and importance of the measurement was stressed. In the context of obtaining new information about transverse GPDs we note that both for σ_L and σ_{LT} there is no twist-2 and twist-3 interference. Given that the form factor R_A^P contributing to twist-2 part is not unknown at large $(-t)$, one could thus obtain the information on the S_T form factor and gain knowledge on H_T GPD. Furthermore, σ_{TT} that is suppressed for DVMP could be used in WA limit to obtain the information on S_S and thus on completely unknown transversity GPD $\tilde{H}_T$.

As often the spin-dependent observables offer additional insight which is less sensitive to particular parameters. For meson photoproduction the most interesting are the correlations of the helicities of the photon and that of either the incoming or the outgoing nucleon, *i.e.*, A_{LL} and K_{LL}, respectively. It can be shown that

$$A_{LL}^{P,tw2} = K_{LL}^{P,tw2},$$
$$A_{LL}^{P,tw3} = -K_{LL}^{P,tw3}, \qquad (7)$$

and so the measurement of A_{LL} and K_{LL} offers characteristic signature for dominance of twist-2 or twist-3. This is similar to the role that the comparison of σ_T and σ_L has in DVMP. From Fig. 4 it is clear that our numerical results suggest the dominance of twist-3 for large θ, while twist-2 increases in the forward direction.

4. Conclusions

In this work we have summarized the recent application of the handbag factorization to WA photo- and electroproduction of pions [16]. In contrast to WACS, but like DVMP, the leading twist-2 analysis which involves helicity non-flip GPDs fails for WA photoproduction by order of magnitude. We have obtained the twist-3 prediction for WAMP which includes both 2- and 3-body twist-3 Fock components of the pions. The π^0 photoproduction was fitted to the data [15] Interesting helicity correlations show that twist-3 dominates for π^0 channel, and mostly for $\pi^\pm$, while in latter case twist-2 matters in forward hemisphere. Different combinations of form factors along with available data should allow to extract the form factors and to learn about large $-t$ behaviour of transversity GPDs important for parton tomography. The application to other pseudoscalar mesons [19] is straightforward.

Acknowledgments

This publication is supported by the Croatian Science Foundation project IP-2019-04-9709, by the EU Horizon 2020 research and innovation programme, STRONG-2020 project, under grant agreement No 824093 and by Deutsche Forschungsgemeinschaft (DFG) through the Research Unit FOR 2926, "Next Generation pQCD for Hadron Structure: Preparing for the EIC", project number 40824754.

---

i. The GPDs $\tilde{E}$ and $\tilde{E}_T$ and their associated form factors decouple at zero skewness.

ii. Twist-3 effects can also be generated by twist-3 GPDs. However, these are expected to be small and therefore neglected.

1. J. C. Collins and A. Freund, Proof of factorization for deeply virtual Compton scattering in QCD, *Phys. Rev. D* **59** (1999) 074009, https://doi.org/10.1103/PhysRevD.59.074009.

2. J. C. Collins, L. Frankfurt and M. Strikman, Factorization for hard exclusive electroproduction of mesons in QCD, *Phys. Rev. D* **56** (1997) 2982, https://doi.org/10.1103/PhysRevD.56.2982.

3. A. V. Radyushkin, Nonforward parton densities and soft mechanism for form-factors and wide angle Compton scattering in QCD, *Phys. Rev. D* **58** (1998) 114008, https://doi.org/10.1103/PhysRevD.58.114008.

4. M. Diehl, T. Feldmann, R. Jakob and P. Kroll, Linking parton distributions to form-factors and Compton scattering, *Eur. Phys. J. C* **8** (1999) 409, https://doi.org/10.1007/s100529901100.

5. H. W. Huang and P. Kroll, Large momentum transfer electroproduction of mesons, *Eur. Phys. J.* **C17** (2000) 423, https://doi.org/10.1007/s100520000500.

6. A. Airapetian *et al.* [HERMES], Single-spin azimuthal asymmetry in exclusive electroproduction of pi+ mesons on transversely polarized protons, *Phys. Lett. B* **682** (2010) 345, https://doi.org/10.1016/j.physletb.2009.11.039.

7. I. Bedlinskiy *et al.* [CLAS], Measurement of Exclusive π^0 Electroproduction Structure Functions and their Relationship to Transversity GPDs, *Phys. Rev. Lett.* **109** (2012) 112001, https://doi.org/10.1103/PhysRevLett.109.112001.

8. M. Defurne *et al.* [Jefferson Lab Hall A], Rosenbluth separation of the π^0 electroproduction cross section, *Phys. Rev. Lett.* **117** (2016) 262001, https://doi.org/10.1103/PhysRevLett.117.262001.

9. M. Dlamini *et al.* [Jefferson Lab Hall A], Deep Exclusive Electroproduction of $\pi 0$ at High Q2 in the Quark Valence Regime, *Phys. Rev. Lett.* **127** (2021) 152301 https://doi.org/10.1103/PhysRevLett.127.152301.

10. S. V. Goloskokov and P. Kroll, An Attempt to understand exclusive pi+ electroproduction, *Eur. Phys. J. C* **65** (2010) 137, https://doi.org/10.1140/epjc/s10052-009-1178-9.

11. M. C. Kunkel *et al.* [CLAS], Exclusive photoproduction of π^0 up to large values of Mandelstam variables s, t and u with CLAS, *Phys. Rev. C* **98** (2018) 015207, https://doi.org/10.1103/PhysRevC.98.015207.

12. R. L. Anderson *et al.*, Measurements of Exclusive Photoproduction Processes at Large Values of t and u from 4-GeV to 7.5-GeV, *Phys. Rev. D* **14** (1976) 679, https://doi.org/10.1103/PhysRevD.14.679.

13. L. Y. Zhu *et al.* [Jefferson Lab Hall A and Jefferson Lab E94-104], Cross section measurements of charged pion photoproduction in hydrogen and deuterium from 1.1-GeV to 5.5-GeV, *Phys. Rev. C* **71** (2005) 044603, https://doi.org/10.1103/PhysRevC.71.044603.

14. H. W. Huang, R. Jakob, P. Kroll and K. Passek-Kumerički, Signatures of the handbag mechanism in wide angle photoproduction of Z pseudoscalar mesons, *Eur. Phys. J. C* **33** (2004) 91, https://doi.org/10.1140/epjc/s2003-01576-6.

15. P. Kroll and K. Passek-Kumerički, Twist-3 contributions to wide-angle photoproduction of pions, *Phys. Rev. D* **97**, no.7 (2018) 074023, https://doi.org/10.1103/PhysRevD.97.074023.

16. P. Kroll and K. Passek-Kumerički, Wide-angle photo- and electroproduction of pions to twist-3 accuracy, *Phys. Rev. D* **104** (2021) 054040, https://doi.org/10.1103/PhysRevD.104.054040.

17. M. Beneke and T. Feldmann, Symmetry breaking corrections to heavy to light B meson form-factors at large recoil, *Nucl. Phys. B* **592** (2001) 3, https://doi.org/10.1016/S0550-3213(00)00585-X.

18. V. M. Braun and I. E. Filyanov, Conformal Invariance and Pion Wave Functions of Nonleading Twist, *Z. Phys. C* **48** (1990) 239, https://doi.org/10.1007/BF01554472.

19. P. Kroll and K. Passek-Kumerički, Wide-angle photoproduction of the η'-meson and its gluon content, *Phys. Rev. D* **105** (2022) 034005 https://doi.org/10.1103/PhysRevD.105.034005.